# WHAT IF…? COMPUTATIONAL ANATOMY IN THE CEREBELLAR MICROZONE, THE MIDDLE LAYER OF THE CEREBELLAR NETWORK

**Mike Gilbert[a] (corresponding author), Anders Rasmussen[b]**

[a]School of Psychology, College of Life and Environmental Sciences, University of Birmingham, Birmingham B15 2TT, UK

ORCID: 0000-0003-4415-6915

[b]Department of Experimental Medical Science, Lund University, BMC F10, 22184 Lund, Sweden

ORCID: 0000-0003-4477-369X

correspondence: m.gilbert.1@bham.ac.uk

## SUMMARY/ABSTRACT

It is generally assumed that the representation of information in the brain is in high resolution and replicable with high fidelity, and that those features make it precise and characterise the inputs to sophisticated computations. Replicability is an important assumption of neural network learning models, including cerebellar models. We question those ideas. The molecular layer of the cerebellar cortex is divided functionally into strips called microzones populated by Purkinje cells and inhibitory interneurons. We propose instead: (1) The microzone computation is a passive effect, unaided, of the triad of cell morphologies, cerebellar network geometry and linear transmission. (2) Control of Purkinje cells is by a chain of rate codes, and not supplanted by learning. (3) Striped topography of input to a network can represent collectively coherent information about body shape and movement. This is capable, passed through the network computation, of driving coordinated motor sequences. (4) A learning algorithm and replicability are unnecessary to explain the evidence.

**Keywords:** cerebellum; theory; hypothesis; model; computational anatomy; cerebellar cortex; molecular layer; microzone; network; middle layer; code

## 1. Introduction

In most vertebrates, the cerebellum makes up 20–30% of the brain by mass and volume. Most of that is the cerebellar cortex, which is divided into an inner and outer layer. Input to the cerebellum is received in the inner layer (granular layer) by granule cells, from mossy fibres. The outer layer, the molecular layer, is divided functionally into long, thin strips called microzones [1-3], which lie at right angles to the axons of granule cells, which are called parallel fibres. Tens of millions of parallel fibres pass through a microzone (Fig 1). Parallel fibres excite both Purkinje cells, which carry the sole output of the cerebellar cortex, and molecular layer interneurons, stellate cells (some vertebrate groups also have basket cells), which in turn inhibit Purkinje cells.

In the classic cerebellar learning model [4-6], the chief instrument of the network computation is the learned modification of parallel fibre synaptic weights. Training causes Purkinje cells to return a learned response to inputs in a pattern received by trained synapses, displacing the naive response to firing rates. Artificial neural networks commonly use synaptic weights similarly, as the main physiological tool of the network computation.

Experimental corroboration of the predicted role of synaptic modification in motor learning remains pending, however [7-10], and naturally-occurring functional graduation of synaptic weights also lacks support [11-13]. There are two further significant evidential issues. One is evidence that rate information is linearly conserved

in signalling between cerebellar neurons [14-17], including synaptic signalling in the molecular layer [18-21], and that cells are adapted for faithful transmission [22-28]. Firing rates linearly code behavioural and task metrics 'at all levels of the cerebellar circuit' [29 p.239, citing 30 references]. It is difficult to reconcile linear transmission with models that use experience to train synaptic weight adjustments, because it is the function of weight changes to displace a rate-coded response.

The second issue is that learning models classically assume that neurally-coded data are replicable – the same data reliably take the same form each time. Replicability is important because signals must be received by the correct set of learned synaptic weights. This assumption may not be safe. Single neurons are not metronomically reliable communicators. Cells are not replicas, even of the same type, and synaptic transmission involves random variables which do not always give the same result, notably release probability, reload speed, and the size of the presynaptic pool of vesicles that are readily releasable.

We present a 'what if?' scenario. We float the idea that anatomy of the molecular layer executes a computational function unaided by learned synaptic modification. We have previously proposed that the granular layer – the input layer of the cerebellar network – converts high-dimensional mossy fibre input into a very low-resolution granule cell code [30]. Output of the granular layer conversion is in units of information which have spatial dimensions – topographically-defined strips – mirroring

functional organisation of the molecular layer into microzones [2, 31-33], so the internal code is striped. Information is coded in a form (collectively, in rate statistics) that is independent of the pattern of active cells, which therefore does not need to be replicated. There is no smaller resolution of granule cell encoded information, and in that sense, it is pixelated. It is not the smallest unit of code, however. Below that scale, any random sample of granule cell signals codes the same information (the code is 'homogenised').

If that is correct, it is unexpected, because it would mean there is a huge sacrifice of multi-dimensional input data, counter to the general expectation that more data should mean more powerful computational performance. We propose that organised data loss is a *function* of the cerebellum. This paper covers the part of the network computation performed in the molecular layer: the microzone computation.

A microzone is the middle layer of the cerebellar network. The input layer is the (spacious) region of the granular layer that provides parallel fibre input to it, and the output layer is the group of cells in the deep cerebellar nuclei that receives its output. We argue that, against traditional expectation, control of Purkinje cells is by the granule cell code, and therefore ultimately by mossy fibre rate information received as input to the network. The microzone computation is a passive effect, unaided and unlearned, of the combination of cell morphologies, cerebellar network geometry and linear transmission. We make that argument by

i) computer simulating the conversion of mossy fibre firing rates into Purkinje cell firing rates; and

ii) showing in principle that striped topography of input to a network can represent collectively coherent information about body shape and movement which – passed through the anatomical computation – drives coordinated motor outputs in a model of swimming.

We use the idea (in the granular layer model and in this paper) that the computational units of the cerebellar network are linear and that units randomly sample the afferent data layer. A sampling unit can be a cell, part of a cell or some other structure. Cerebellar code spans the network sagittally. Anatomy mimics random sampling of the whole afferent layer of firing rates, with replacement, notwithstanding that a single unit receives unchanging contact from a tiny fraction of afferent-layer cells. Cell morphologies and network geometry are explicable as bespoke adaptations for this function. Sampling units are not an abstraction or a simplification, but the physical hardware of a computational mechanism – the biological counterpart of parameters of the network computation. In this contention, biology is adapted to isolate the effect of computationally relevant parameters, by eliminating or negating other variables. There are reported examples of exactly this in the cerebellum, where cell-to-cell communication is adapted to control for variables that are not code, i.e., to conserve fidelity of linear transmission of rate information [14-17, 22, 23, 26-28, 34-36].

Variables which code nothing are noise, including biophysical variables. During behaviour, signalling is analogue, and accordingly so is (the biological proxy of) 'sampling' of firing rates.

The network model takes 80,000 inputs, representing concurrent mossy fibre activity supplying information to a network, and returns 400 outputs, representing firing of Purkinje cells in the middle microzone. Synaptic learning is omitted from the discussion because – we propose – it is not involved in the computation. We cover learning separately [ref 'What if…?' learning paper]. In most networks, Purkinje cells are not the output cells of the network, but exert a powerful influence to which output cells are immediately and bi-directionally responsive [37].

Generally, neural network models solve a problem it is proposed the network has. The solution is a computational mechanism; the mechanism is the model. The proposal is an assumption it makes. The direction is function → mechanism (the first two steps of Marr's three levels of analysis). We use modelling in a different role, to quantify and test the ideas by simulating the mechanism, to verify that it works with physiological parameters. We infer function from the mechanism. The direction is mechanism → function. This direction led to the ideas presented here.

## Figure 1

# 2. Hypothesis

## 2.1 The granule cell code

As noted, we have previously modelled recoding in the granular layer which generates the granule cell code [30]. In the traditional learning model, it is implicit that a granule cell code is effectively redundant, because control of Purkinje cells by granule cell rates is displaced by learning. We propose there is a code. Features of the code are:

(i) The same information is collectively coded in the firing rates of any random sample of active parallel fibres at the intersection with a sagittal plane. The intersection with a microzone approximates a sagittal plane.

(ii) The code spans a network so that a whole microzone receives, at any moment, the same code. The form of the code is the frequency distribution of firing rates.

(iii) It is immaterial (codes nothing) which parallel fibres are active, in what pattern, or what rates they each fire at, or even what rates those are (subject to statistical constraints on the frequency distribution).

## 2.2 The microzone mechanism

Firing rates in a snapshot of parallel fibre activity at the intersection with a microzone represent a data set. Purkinje cells and stellate cells each receive contact from what is,

functionally speaking, a random sample of passing parallel fibres, and therefore a random sample of active cells. Stellate cell firing rates are a linear function of the mean (or sum) of input rates. This generates a second data set, with a narrower distribution and the same (or a linearly related) mean, by the central limit theorem. Purkinje cell dendritic compartments randomly sample stellate cells belonging to the network of stellate cells afferent to the Purkinje cell. Membrane voltage of dendritic compartments is a linear function of the mean firing rate of stellate cells afferent to the compartment. The Purkinje cell firing rate linearly codes the mean of the sample means, i.e., averaged compartment voltages. The sample means constitute a third data set. The statistical effect is the same as before – the range is further narrowed and the mean is some linear function of the mean of the sampled distribution, this time stellate cell rates. The result is that parallel fibre rates (derived by the granular layer model) are converted to coherent (i.e. narrowly focussed) Purkinje cell firing rates whose mean is precisely and reliably predicted by the granule cell code. As the granule cell code is predicted by mossy fibre rates, Purkinje cell firing is predicted by mossy fibre rates. References to Purkinje cells in this description are to the population of a microzone (hundreds), the middle layer of the cerebellar network, and references to granule cells are to the population of the input layer (millions).

## 3. Terminology

A note on terminology. We divide the input layer of a network into nominal (200 x 150 µm, Fig 1) 'fields'. These are simply a device. They are not anatomically or indeed even functionally distinct or separate. A row of fields that spans the input layer sagittally is a 'rank' (a rank has the dimensions of a microzone seen from the cerebellar surface). A row that spans the input layer mediolaterally (therefore at right angles to ranks and microzones) is a 'file'. The microzone that equally bisects the input layer is the 'middle microzone'. Like fields, division into files is simply a device to quantify the ideas, and does not reflect physiological segregation of information. Figure 1 illustrates our terminology.

## 4. Basis to assume the density of active parallel fibres is low and uniform

There is a long-standing prediction for theoretical reasons that the fraction of parallel fibres that are active at any time is regulated [5], fixed [4], and low (termed sparse code). Granule cells typically fire in short bursts [20, 38, 39]. However, there is a constant high turnover of active cells. The physiological density remains unknown.

We disagree with the traditional reasons, but agree the code is sparse, for these reasons. i) Low density is stable (Fig 2). Randomly fluctuating density would be noise. Stability may be enhanced by feedback via granule cell ascending axon contact on Golgi cell basal dendrites [24] and parallel fibre contact on Golgi cell apical dendrites, acting partly through gap junctions [40]. ii) Low density is energy efficient. Granule cells are very numerous and they are not myelinated (so spike propagation is costly). iii) The reported number of coincidentally active inputs to a stellate cell is in single figures [41], consistent with low density of co-active parallel fibres (see Table A). iv) It is thought that the pattern of active and inactive parallel fibres, and the pattern in which firing rates are distributed among active cells, are decorrelated – effectively, quasi-randomised. Low density enhances practical decorrelation, that is, if decorrelation is not perfectly random – as it may not be [42] – low density increases the randomness of the pattern of synaptic activations received by targets.

We modelled regulation of parallel fibre density (Fig 2). Previously, we modelled a single rank [30]. Here, we extend that to the whole input layer of a network, based on a 3 mm range of parallel fibres in each direction from the soma [43, 44] and a microzone dimensions of 150 µm x 2,000 µm viewed from the cerebellar surface (estimates and probably actual dimensions vary [2, 3, 45]). A region of that size is crossed by 41 ranks, 20 either side of the middle microzone and one directly beneath (Fig 1). Outputs of the model are the number of granule cells that fire in each field and the rates they fire at. As we know the number of active granule cells in each field, we

know the number in each file. The number of active parallel fibres at the intersection of a file with the middle microzone is the sum of active granule cells in that file. Local regulation of the number of active granule cells in each field becomes still tighter regulation of the number of active parallel fibres in a file, a statistical effect of cerebellar cortical architecture (Fig 2, 3$^{rd}$ and 6$^{th}$ columns). The range is narrow regardless of the frequency distribution of mossy fibre rates. At low density, the regulated density of active parallel fibres is hyper focussed.

Local feedback via the granule cell ascending axon [24, 46] may condense the physiological range of field-to-field variation (and therefore also file-to-file variation). Feedback via parallel fibres [4, 40] would (additionally) reduce the range of file-to-file variation. These are not represented in the simulation.

By our calculations (Fig 2), parallel fibre density is uniform and invariant at the scale of the intersection of a microzone and a file. Below that scale, random distribution of active cells among the general population is an assumption. In fact, the pattern of active cells may not be fully random at this level. Clustered patterns of parallel fibre activity have been reported (with calcium imaging) [42]. However, parallel fibre targets receive contact from only a fraction of parallel fibres that pass nearby, around one in eighty for stellate cells and one in two for Purkinje cells [47]. The number of signals that are received by Purkinje cells is effectively further reduced because most parallel fibre synapses on Purkinje cells are severely depressed [11, 12]. So if clustering occurs,

it is likely to be absent from the pattern of signals that are received by targets at working (i.e., not silent) synapses.

**Figure 2**

## 5. Stellate cells receive an 'independent' random sample of parallel fibre rates

In our proposal, the cerebellum exploits statistical effects that depend on the independence of random samples. Cerebellar cortical architecture simulates independence. The granular layer model also returns the firing rates of granule cells in each field, and therefore the frequency distribution of parallel fibre rates in each file, and so rates received by each sector of the middle microzone. All sectors receive the same or a narrowly varying distribution (Fig 3 rows 1 and 3, column 3, are randomly selected examples). Like density, this result is unaffected by the frequency distribution of mossy fibre rates. Accordingly, all targets in a plane at right angles to parallel fibres sample, at any instant, the same distribution, a biological proxy of sampling the entire population of input rates to a microzone with replacement.

To test (by simulating it) if anatomy could in theory have the computational effect we propose, we first need the number of inputs to a stellate cell that are active at any time: sample size. The stellate cell territory is sagittally flattened in the plane orthogonal to parallel fibres. Stellate cells form planar networks [48] that occupy the space (about 40 µm) between Purkinje cells [49]. An estimated 350,000 parallel fibres pass through the Purkinje cell dendritic arbour [47]. The Purkinje cell dendritic territory measures ~300 x 200 µm in the sagittal plane, the target presented to parallel fibres. The stellate cell dendritic territory is smaller and varies with the depth of the cell body in the molecular layer. For superficially located ('outer-level') cells it is around 80 x 80 µm. At deeper level ('inner level') it is larger, around 120 x 120 µm [49 pp.217-221]. Therefore, ~84,000 parallel fibres pass through an inner-level territory, given by 350,000/((200x300)/$120^2$), assuming parallel fibres are uniformly distributed. If 0.5% are active in the general population, around 420 of those are active.

It has been estimated that a stellate cell receives contact from several hundred parallel fibres [49, 50], which we take as 1,000. Working with these estimates, 1 in 84 make contact (i.e., 1,000 out of 84,000), so the probability that an active cell makes contact is 1/84 = ~0.0119. Accordingly, contact by $x$ (out of 420) active cells has a probability given by

$$\frac{420!}{x!\,(420-x)!} * 0.0119^{x} * (1-0.0119)^{420-x}$$

Probabilities are shown in Table A for the range $x$ = 0 to 12, where $x$ is the number of active parallel fibres that make contact and $p$ is the probability of that number. The distribution of probabilities is in good agreement with the modest number – single figures – suggested by 'two to eight substantial EPSPs' [41 p.9628].

**Table A** The probability, $p$, that a stellate cell receives contact from $x$ active parallel fibres

| $x$ | 0 | 1 | 2 | 3 | 4 | 5 | 6 | 7 | 8 | 9 | 10 | 11 | 12 |
|---|---|---|---|---|---|---|---|---|---|---|---|---|---|
| $p$ | .0066 | .0331 | .0836 | .1403 | .1762 | .1765 | .147 | .1047 | .0651 | .0359 | .0178 | .008 | .0033 |

There are an estimated 16 stellate cells for each Purkinje cell [51], meaning 80 stellate cells per field (there are four Purkinje cells per field so five layers of stellate cells are needed to inhibit them from both sides). As noted, parallel fibre rates in each file were obtained by pooling granule cell rate data for fields in that file. Sample size was randomly generated with the probabilities in Table A. This gave the number of active inputs, and input rates, to each stellate cell in the middle microzone (Fig 3D).

As far as we know, there are no data for the conversion of multiple input rates into changes of the stellate cell firing rate, although it is some linear function [20]. We assume that stellate cell firing is a linear function of the mean of input rates, which we take to be the mean itself (the sum works as well). This is not to suggest that stellate

cell firing rates are equal to the mean of input rates, but that they scale proportionally with the mean.

Speaking generally, rate information transitions through multiple biophysical steps even in transit through a single neuron. Normally, these are measured on different scales. Scales are arbitrary *per se* but bring consistency to data collection. For our purpose – to demonstrate a computational effect of anatomical parameters – it is unnecessary to know the conversion function (except that it is linear), so a common scale suffices.

The result is a new data set with a smaller range and the same mean as granule cell rates. The true relationship of the means is the same as the function that relates the stellate cell firing rate to the mean of input rates.

## 6. Purkinje cell dendritic compartments receive innervation from an independent random sample of stellate cells

A microzone is ~100 Purkinje cells long and 4 wide (400 is consistent with reported convergence and divergence ratios onto 50 deep cerebellar nuclear cells [rats: 52]. In our simulation, a field contains 4 Purkinje cells. A Purkinje cell receives contact from stellate cells from both of its flat sides, ~16 each side, and a smaller number of stellate

cells in the two sagittally-neighbouring fields. Inhibition from neighbouring fields is from a smaller number of stellate cells because not all of them extend their main axon far enough to reach, and some of them extend their main axon the wrong way. We represent those conditions as variables in the simulation. The vertical range of stellate cell axon collaterals and the horizontal range of the main axon both increase with the depth of the cell body in the molecular layer [49, 53]. Because of their more limited horizontal range, outer-level stellate cells are excluded in the simulation from contacting Purkinje cells in neighbouring fields.

The planar Purkinje cell arbour is large and branches profusely, and stellate cell contact is dispersed across it. We divide the Purkinje cell arbour nominally into sixteen 50 x 75 µm compartments. For morphological reasons, input to a compartment is not confined to (or even necessarily always received from) the nearest stellate cells, but each compartment is in range of the majority of the afferent network. As a result, each compartment receives contact from a random sample of stellate cells afferent to a Purkinje cell.

It is unknown how many stellate cells innervate a nominal Purkinje cell compartment. We take it as 5, ~20% of the stellate cell network afferent to a Purkinje cell, selected to be conservative (and therefore hypothesis neutral), and that local dendritic membrane potential is a linear function of the mean of input rates. Sampling is independent of sampling by other compartments, i.e., innervation of a compartment

320 by a stellate cell does not exclude innervation by the same cell of other compartments.
321 Taking the sample means gives 6,400 values made up of 400 data sets, one for each
322 middle-microzone Purkinje cell (Fig 3G).

323 Interneuron firing rates linearly reflect granule cell input [20]. Disynaptic inhibition via
324 interneurons causes the firing rate of Purkinje cells in slices to decrease as a linear
325 function of the strength of granule cell firing [21]. As there is also a linear relationship
326 of Purkinje cell firing and direct synaptic excitation (with inhibitory synaptic
327 transmission blocked) [18, 19], we took the sample means to be linearly related to
328 compartment membrane voltage.

329 A Purkinje cell receives inhibition from two stellate cell networks, one each side. We
330 repeated the steps above for the other flanking network, then took the mean for each
331 compartment. Output of this step is again 400 sets of 16 values (Fig 3H).

332 Stellate cells contact Purkinje cells on smooth dendrites [49]. In self-paced mice,
333 recording from smooth dendrites, 'Locomotion-dependent modulation of the balance
334 between excitation and inhibition generates depolarising or hyperpolarising dendritic
335 $V_m$ [dendritic membrane voltage] changes that linearly transform into bidirectional
336 modulation of PC SSp [Purkinje cell simple spike] output' [20 p.9]. Smooth dendrites
337 extend into all compartments, mitigating the effect of filtering and distance on
338 dendritic signalling. We take Purkinje cell somatic polarisation as the mean of the
339 compartment means. The result is a new data set with a still further narrowed range. A

linear statistical relationship between input (the granule cell code) and output (Purkinje cell firing) of the microzone computation is conserved. Since granule cell firing linearly encodes mossy fibre rates, there is a linear relationship of Purkinje cell rates and mossy fibre rates. The new data are again on a normalised scale. Coded this way, a short sequence of computational steps is sufficient to focus an input range of hundreds of Hz down to a few Hz which is precisely predicted by mossy fibre rates upstream (Fig 3I and J).

We argue here that the function of the computation becomes evident in context. We use the Discussion section to propose context.

**Figure 3**

## 7. Discussion

### What if…? Cerebellar networks are functionally paired with muscles

The cerebellum is not confined to an indirect influence on movement, as at one time it was thought. Cerebellospinal neurons provide 'a direct link between the cerebellum and spinal substrates for motor coordination' in mice [54]. The output pathway is

reciprocated by spinocerebellar neurons, providing a substrate for direct motor control, which spinal locomotor networks alone cannot accomplish reliably or with finesse [55].

The vertebrate cerebellum first appeared in a marine environment. It is probably not contentious that early swimming, before efficient teleosts, was anguilliform. Modern agnathans, the nearest extant relative of a common vertebrate ancestor, swim in this way, although it is not clear if divergence of extant agnathans from the main vertebrate line came before or after the appearance of a proper cerebellum. Modern hagfish, for example, don't have a proper cerebellum, but there is evidence (from gene expression in prenatal development) that their ancestors once did [56].

Almost the entire musculature of fish is made up of a bilaterally symmetrical row of paired axial muscle segments, termed myomeres. Movement through the water is produced by a repeating sequence of muscle contractions which cause lateral body flexion. The preferred method of most fish is to generate thrust from a sagittally-flattened tail. But in an earlier form, undulating swimming was probably eel-like (anguilliform), using alternating left and right head turns to set up a herring-bone pattern of high pressure which the animal rides by making itself an undulating shape.

Muscles generate information constantly, in muscle spindles, specialised muscle fibres. There are three types of muscle spindle fibres, two firing at rates proportional to muscle length, and the third signalling the rate of change of muscle length. Group II

afferent neurons innervate the first two so they signal muscle length. Group Ia afferent neurons innervate all three, so they fire at a rate that varies with muscle length but in addition varies proportionally to the rate of muscle extension and (more modestly) inversely proportionally to the rate of muscle contraction. Lateral flexion of the trunk during swimming causes muscle fibre length to vary sinusoidally, and therefore generates sinusoidally varying signal frequencies. The rate of change of muscle fibre length is therefore also sinusoidal since it is the derivative (the slope of a tangent to a sinusoidal waveform, derived by differentiation, is itself a sine wave).

We propose that in a vertebrate ancestor, input to a row of topographically-defined strips of the granular layer (ranks) arose from a corresponding row of contralateral myomeres. Neighbouring myomeres send their output to neighbouring ranks. During locomotion, at any moment, a graph of mossy fibre input rates to the input layer of a network – 40 or so ranks in our model – is therefore a sine wave or part of a sine wave (Figs 4 and 5). In the next moment, the wave advances slightly. The size of the portion of a sine wave represented by a snapshot of input to a network depends on the number of muscle segment pairs that fit into a full body wave. Phase by phase, input to a single rank passes through the same cycle. Input to neighbouring ranks is a small step out of phase.

Output of a network is ipsilateral and to a single myomere, opposite the middle of the row that provides input. A network is therefore the junction of multiple input

pathways and a single output pathway. Neighbouring networks connected by parallel fibres send output to neighbouring myomeres. This connectivity is mirrored in the contralateral cerebellum, which has motor output to the other half of the body.

**Figure 4**

## Why would that generate smoothly modulated motor outputs with exactly coordinated timing?

The cerebellum contributes smooth execution and precise coordination to movements. The physiological model of swimming will do that if the cerebellum performs the computation we have proposed.

The granular layer computation converts high-dimensional mossy fibre input to the cerebellum into a very low-resolution granule cell code [30]. Granule cell-encoded information is indivisible in long strips of the granular layer, which we liken to pixels. The pixellated granule cell code is literally short-lived. Pixels only retain their integrity – i.e., pixel codes are only segregated – in granule cell ascending axons, while signals travel towards the cerebellar surface. Beyond that, after the granule cell axon divides in two, parallel fibre signals are randomly mixed up, within modal strata [38, 49, 57].

On the face of it, this only seems to spectacularly compound the loss of data. We propose that hyper-conflation of data is a *function* of data processing. There is fossil evidence of a proto-chordate with almost vertical muscle segments [58]. Modern adult fish have nested W-shaped myomeres with the centre pointing forwards [59]. The W shape spreads the force transmitted to the skeleton by muscle contractions. It also helps to reduce the forces acting on collagen membranes called myosepta which separate myomeres. Myomeres, like skeletal muscle generally, are made up of muscle fibres. Muscle fibres are anchored at both ends to myosepta. Fibres are angled towards horizontal so that the force acting perpendicular to the myoseptum is less than the force of the contraction, without weakening the force that bends the body [60]. Analysis of the 3-dimensional pattern of fish muscle fibre angles is complex [61]. One interpretation is that they are arranged so that they contract 'to a fairly similar extent when the fish bends', delivering more power than contraction by different amounts [62].

Speaking generally, it is well established that neuron performance is noisy – there is inherent biological variability from cell to cell and even of firing of the same cell at different times in the same conditions. We might suppose, therefore, that firing rates which code the length of muscle fibres, and the rate they change length, are to some degree randomly variable. Also, muscle fibres that are differently angled, or different lengths, may not change length by the same amount or at the same rate.

The biological solution – we suggest – is to compound the data: averaging. Output of a myomere is pooled for this purpose. This can't be done at spinal level so it goes through the cerebellum. Input to the cerebellum from muscle fibres in a myomere, received by a granular layer rank, is accordingly handled with disregard for resolution below a topographically-defined scale, and converted to the pixel code. Pixel codes are in turn averaged by the microzone computation. The network computation distils a single output rate, or a narrow, normally-distributed range that approaches a single output rate. Output is sent to motor neurons. 'Motor neurons are clustered in columnar, spinal nuclei called motor neuron pools (or motor nuclei). All of the motor neurons in a motor neuron pool innervate a single muscle, and all motor neurons that innervate a particular muscle are contained in the same motor neuron pool. Thus, there is a one-to-one relationship between a muscle and a motor neuron pool.'[1] Axons of spinal neurons that innervate and excite a motor neuron pool branch terminally, making contact indiscriminately on neurons inside.

This permits a one-to-one relationship of a cerebellar network and a motor pool, and through a motor pool, a myomere. Graded control of muscle fibres is provided because motor neurons are different sizes (in mammals there are three sizes). Each step up in size selectively innervates more powerfully contractile (but more exhaustible) muscle fibres. Larger motor neurons require stronger depolarising current to fire, so weak input signals excite only small motor neurons and the least powerful muscle fibres.

[1] Reproduced with permission by McGovern Medical School, University of Texas

Stronger signals cause more motor neurons to be recruited, including larger ones, and therefore more muscle fibres, including fibres that contract with more force.

In anguilliform swimming, a wave of muscle extension passes down each side of the body, 180 degrees out of phase. Signals representing muscle fibre length and rate of extension are streamed to the contralateral cerebellum, where they are received by a corresponding set of topographically-defined units of the cerebellar cortex, which we term ranks. Conflated pixel codes provide parallel fibre drive to microzones. This is passed through the microzone computation to distil a single output rate. Each microzone sends its output, a single firing rate, to an ipsilateral motor neuron pool, which in turn controls a myomere. By this pathway, contralateral muscle fibre extension drives proportional ipsilateral muscle contractions. Bending of the body drives a spiral of inputs and outputs that passes along a row of networks, causing a wave of contractions to pass backwards along the body. Alternating left and right head turns initiate backwards propagating waves 180 degrees out of phase, assisted by passive undulation.

It is a long-standing puzzle why neighbouring microzones share such a high percentage of parallel fibre inputs. In fact, next door neighbouring microzones receive almost *all* of the same parallel fibre inputs (~97.5% assuming a microzone span of 150 µm). In the present proposal, this has a function. Granule cell-coded parallel fibre input to immediately neighbouring microzones is very closely in step because input is almost all

the same. Output is therefore also coordinated, with equal precision, because output is controlled by the granule cell code. Coordination is in this way automated, simply the outcome of anatomy. The same relationship exists with more distant neighbours of a network in both directions to a degree that is inversely related to the distance. Output is streamed, so coordination of output rates provides coordination of the timing of motor outputs and automates smooth execution of performance.

This comes with a problem. For precision, input to a microzone must be exactly phase-sensitive. The input layer of the cerebellar network receives inputs from a row of contralateral muscle segments, diluting phase-secificity. Taken to an extreme, if the number of segments providing signals is the same as the number in a full wave of the body, the information is perfectly imprecise – there is no phase information at all (Fig 4). However, if muscle segments are thin, so that signals informing motor output originate in a smaller length of the body relative to wavelength, phase information emerges. The lower the ratio (of sector length to wavelength), the more precise it is (Fig 5).

There are in addition at least two strategies that focus a phase-specific response. In the first, there is a gradient, with granule cell signals originating nearby having more influence. Parallel fibres make about half as many synapses distally than proximally, and swellings where contact is made contain fewer synaptic densities [63]. As a result,

there is a stronger influence of nearer granule cells, and therefore upstream of mossy fibre signals originating in nearer myomeres.

The second is a result of granule cell T-shaped morphology. *Used in middle layer II* [Purkinje cells receive significant granule cell ascending axon contact [64]. Ascending axon synapses on Purkinje cells are resistant to modification, and have low uncertainty of release probabilities [65].] Mossy fibre input to the middle rank of a network is sourced from the antagonist of the myomere which receives the output of the network. Accordingly, excitation of Purkinje cells receives phase weighting from ascending axons of directly underlying granule cells.

A feature we like is that parallel fibres of standard length maintain the amplitude of body undulations as they pass backwards. This is efficient because the whole body rides the herringbone pattern of high pressure, not achieved by caudally diminishing amplitude of passive undulations.

So, it is a function of the cerebellum to discard input resolution below a topographically-defined scale in order to take an average of muscle fibre data, and then to average that data with data from other muscles. This allows the cerebellum – indeed, it is purposed – to process input data blind below the same scale, and even though data may be individually imprecise (because performance of single cells can be variable). It is unnecessary for the neural form of data to be replicable or indeed for patterns to ever be repeated. Parallel fibres finely coordinate the relative strength of

motor outputs between near neighbouring networks, and time-varying modulation of the strength of outputs is automatically phase commensurate. All this needs only simple executive input (head turns).

In most networks, Purkinje cells are not the output cells of the network, but exert a powerful influence to which output cells are immediately and bi-directionally responsive [37]. We cover the deep cerebellar nuclei separately [ref 'What if…?' output layer paper].

**Figure 5**

## Grants

Funding: This work was supported by the Leverhulme Trust [grant number ECF-2022-079] (Mike Gilbert); the Swedish Research Council [grant number 2020-01468]; the Per-Eric och Ulla Schybergs Foundation [grant number 42630]; and the Crafoord Foundation [grant numbers 20180704, 20200729, 20220776, & 20230655] (Anders Rasmussen).

## Author contributions

M.G. Researched, conceived and developed the ideas, performed the analysis, wrote the code, prepared the figures and wrote the manuscript. A.R. provided expertise and feedback, and reviewed and provided editorial comments on the manuscript.

## Declaration of interests

The authors declare no competing interests.

## REFERENCES


1. Garwicz, M., C.F. Ekerot, and H. Jorntell, *Organizational principles of cerebellar neuronal circuitry.* News in Physiological Sciences, 1998. **13**: p. 28-34.
2. Oscarsson, O., *Functional units of the cerebellum - sagittal zones and microzones.* Trends in Neurosciences, 1979. **2**: p. 143-145.
3. Ozden, I., et al., *Reliable coding emerges from coactivation of climbing fibers in microbands of cerebellar Purkinje neurons.* J Neurosci, 2009. **29**(34): p. 10463-73.
4. Albus, J.S., *A Theory of Cerebellar Function.* Mathematical Biosciences, 1971. **10**(1-2): p. 25-61.
5. Marr, D., *A theory of cerebellar cortex.* J Physiol, 1969. **202**(2): p. 437-70.
6. Fujita, M., *Adaptive filter model of the cerebellum.* Biol Cybern, 1982. **45**(3): p. 195-206.
7. Welsh, J.P., et al., *Normal motor learning during pharmacological prevention of Purkinje cell long-term depression.* Proc Natl Acad Sci U S A, 2005. **102**(47): p. 17166-71.
8. Schonewille, M., et al., *Reevaluating the role of LTD in cerebellar motor learning.* Neuron, 2011. **70**(1): p. 43-50.
9. ten Brinke, M.M., et al., *Evolving Models of Pavlovian Conditioning: Cerebellar Cortical Dynamics in Awake Behaving Mice.* Cell Rep, 2015. **13**(9): p. 1977-88.
10. Boele, H.-J., et al., *Impact of parallel fiber to Purkinje cell long-term depression is unmasked in absence of inhibitory input.* Science Advances, 2018. **4**(10).
11. Isope, P. and B. Barbour, *Properties of unitary granule cell-->Purkinje cell synapses in adult rat cerebellar slices.* J Neurosci, 2002. **22**(22): p. 9668-78.
12. Ekerot, C.F. and H. Jörntell, *Parallel fibre receptive fields of Purkinje cells and interneurons are climbing fibre-specific.* Eur J Neurosci, 2001. **13**(7): p. 1303-10.
13. Hesslow, G., et al., *Classical conditioning of motor responses: what is the learning mechanism?* Neural Netw, 2013. **47**: p. 81-7.
14. Rancz, E.A., et al., *High-fidelity transmission of sensory information by single cerebellar mossy fibre boutons.* Nature, 2007. **450**(7173): p. 1245-8.
15. Ritzau-Jost, A., et al., *Ultrafast action potentials mediate kilohertz signaling at a central synapse.* Neuron, 2014. **84**(1): p. 152-163.
16. Duguid, I., et al., *Control of cerebellar granule cell output by sensory-evoked Golgi cell inhibition.* Proc Natl Acad Sci U S A, 2015. **112**(42): p. 13099-104.
17. Duguid, I., et al., *Tonic inhibition enhances fidelity of sensory information transmission in the cerebellar cortex.* J Neurosci, 2012. **32**(32): p. 11132-43.
18. Walter, J.T. and K. Khodakhah, *The linear computational algorithm of cerebellar Purkinje cells.* J Neurosci, 2006. **26**(50): p. 12861-72.
19. Walter, J.T. and K. Khodakhah, *The advantages of linear information processing for cerebellar computation.* Proc Natl Acad Sci U S A, 2009. **106**(11): p. 4471-6.
20. Jelitai, M., et al., *Dendritic excitation-inhibition balance shapes cerebellar output during motor behaviour.* Nat Commun, 2016. **7**: p. 13722.
21. Park, S.M., E. Tara, and K. Khodakhah, *Efficient generation of reciprocal signals by inhibition.* J Neurophysiol, 2012. **107**(9): p. 2453-62.

22. Delvendahl, I. and S. Hallermann, *The Cerebellar Mossy Fiber Synapse as a Model for High-Frequency Transmission in the Mammalian CNS.* Trends Neurosci, 2016. **39**(11): p. 722-737.
23. Saviane, C. and R.A. Silver, *Fast vesicle reloading and a large pool sustain high bandwidth transmission at a central synapse.* Nature, 2006. **439**(7079): p. 983-7.
24. Cesana, E., et al. *Novel granule cell-Golgi cell excitatory input in the cerebellar granular layer*. in *FENS Abstr*. 2010.
25. Moore, J.W. and D.E.J. Blazis, *11 - Simulation of a Classically Conditioned Response: A Cerebellar Neural Network Implementation of the Sutton–Barto–Desmond Model*, in *Neural Models of Plasticity*, J.H. Byrne and W.O. Berry, Editors. 1989, Academic Press. p. 187-207.
26. Sargent, P.B., et al., *Rapid vesicular release, quantal variability, and spillover contribute to the precision and reliability of transmission at a glomerular synapse.* J Neurosci, 2005. **25**(36): p. 8173-87.
27. Turecek, J., S.L. Jackman, and W.G. Regehr, *Synaptic Specializations Support Frequency-Independent Purkinje Cell Output from the Cerebellar Cortex.* Cell Reports, 2016. **17**(12): p. 12.
28. Turecek, J., S.L. Jackman, and W.G. Regehr, *Synaptotagmin 7 confers frequency invariance onto specialized depressing synapses.* Nature, 2017. **551**: p. 503.
29. Raymond, J.L. and J.F. Medina, *Computational Principles of Supervised Learning in the Cerebellum.* Annu Rev Neurosci, 2018. **41**: p. 233-253.
30. Gilbert, M. and A. Rasmussen, *What if...? Computational anatomy in the granular layer of the cerebellar cortex.* bioRxiv, 2024: p. 2023.07.14.548987.
31. Andersson, G. and O. Oscarsson, *Climbing fiber microzones in cerebellar vermis and their projection to different groups of cells in the lateral vestibular nucleus.* Exp Brain Res, 1978. **32**(4): p. 565-79.
32. Groenewegen, H.J. and J. Voogd, *The parasagittal zonation within the olivocerebellar projection. I. Climbing fiber distribution in the vermis of cat cerebellum.* J Comp Neurol, 1977. **174**(3): p. 417-88.
33. Groenewegen, H.J., J. Voogd, and S.L. Freedman, *The parasagittal zonation within the olivocerebellar projection. II. Climbing fiber distribution in the intermediate and hemispheric parts of cat cerebellum.* J Comp Neurol, 1979. **183**(3): p. 551-601.
34. DiGregorio, D.A., et al., *Desensitization properties of AMPA receptors at the cerebellar mossy fiber granule cell synapse.* J Neurosci, 2007. **27**(31): p. 8344-57.
35. Mapelli, L., S. Solinas, and E. D'Angelo, *Integration and regulation of glomerular inhibition in the cerebellar granular layer circuit.* Front Cell Neurosci, 2014. **8**: p. 55.
36. Galliano, E., P. Mazzarello, and E. D'Angelo, *Discovery and rediscoveries of Golgi cells.* J Physiol, 2010. **588**(Pt 19): p. 3639-55.
37. Pedroarena, C.M. and C. Schwarz, *Efficacy and short-term plasticity at GABAergic synapses between Purkinje and cerebellar nuclei neurons.* J Neurophysiol, 2003. **89**(2): p. 704-15.
38. Jörntell, H. and C.F. Ekerot, *Properties of somatosensory synaptic integration in cerebellar granule cells in vivo.* J Neurosci, 2006. **26**(45): p. 11786-97.

39. van Beugen, B.J., et al., *High Frequency Burst Firing of Granule Cells Ensures Transmission at the Parallel Fiber to Purkinje Cell Synapse at the Cost of Temporal Coding.* Frontiers in Neural Circuits, 2013. **7**: p. 95.
40. Gilbert, M. and A. Rasmussen, *Gap Junctions May Have A Computational Function In The Cerebellum: A Hypothesis.* The Cerebellum, 2024.
41. Jörntell, H. and C.F. Ekerot, *Receptive field plasticity profoundly alters the cutaneous parallel fiber synaptic input to cerebellar interneurons in vivo.* J Neurosci, 2003. **23**(29): p. 9620-31.
42. Wilms, C.D. and M. Häusser, *Reading out a spatiotemporal population code by imaging neighbouring parallel fibre axons in vivo.* Nature Communications, 2015. **6**: p. 6464.
43. Brand, S., A.L. Dahl, and E. Mugnaini, *The length of parallel fibers in the cat cerebellar cortex. An experimental light and electron microscopic study.* Exp Brain Res, 1976. **26**(1): p. 39-58.
44. Mugnaini, E., *The length of cerebellar parallel fibers in chicken and rhesus monkey.* J Comp Neurol, 1983. **220**(1): p. 7-15.
45. Ramirez, J.E. and B.M. Stell, *Calcium Imaging Reveals Coordinated Simple Spike Pauses in Populations of Cerebellar Purkinje Cells.* Cell Reports, 2016. **17**(12): p. 3125-3132.
46. Cesana, E., et al., *Granule cell ascending axon excitatory synapses onto Golgi cells implement a potent feedback circuit in the cerebellar granular layer.* J Neurosci, 2013. **33**(30): p. 12430-46.
47. Harvey, R.J. and R.M. Napper, *Quantitative study of granule and Purkinje cells in the cerebellar cortex of the rat.* J Comp Neurol, 1988. **274**(2): p. 151-7.
48. Häusser, M. and B.A. Clark, *Tonic synaptic inhibition modulates neuronal output pattern and spatiotemporal synaptic integration.* Neuron, 1997. **19**(3): p. 665-78.
49. Palay, S.L. and V. Chan-Palay, *Cerebellar cortex : cytology and organization*. 1974, Berlin: Springer.
50. Carter, A.G. and W.G. Regehr, *Quantal events shape cerebellar interneuron firing.* Nat Neurosci, 2002. **5**(12): p. 1309-18.
51. Llinás, R.R. and M.N. Negrello. *Cerebellum*. Scholarpedia, 10(1):4606 2015 [cited 2017 06/01]; Available from: http://www.scholarpedia.org/article/Cerebellum.
52. Person, A.L. and I.M. Raman, *Synchrony and neural coding in cerebellar circuits.* Frontiers in Neural Circuits, 2012. **6**: p. 97.
53. Sultan, F. and J.M. Bower, *Quantitative Golgi study of the rat cerebellar molecular layer interneurons using principal component analysis.* J Comp Neurol, 1998. **393**(3): p. 353-73.
54. Sathyamurthy, A., et al., *Cerebellospinal Neurons Regulate Motor Performance and Motor Learning.* Cell Rep, 2020. **31**(6): p. 107595.
55. Parker, D., *Complexities and uncertainties of neuronal network function.* Philos Trans R Soc Lond B Biol Sci, 2006. **361**(1465): p. 81-99.
56. Sugahara, F., et al., *Genetic Mechanism for the Cyclostome Cerebellar Neurons Reveals Early Evolution of the Vertebrate Cerebellum.* Frontiers in Cell and Developmental Biology, 2021. **9**.

57. Zhang, W. and D.J. Linden, *Calcium influx measured at single presynaptic boutons of cerebellar granule cell ascending axons and parallel fibers.* Cerebellum, 2012. **11**(1): p. 121-31.
58. Morris, S.C. and J.B. Caron, *Pikaia gracilens Walcott, a stem-group chordate from the Middle Cambrian of British Columbia.* Biol Rev Camb Philos Soc, 2012. **87**(2): p. 480-512.
59. Tytell, E., *Fish muscle is still helical.* Journal of Experimental Biology, 2003. **206**(15): p. 2530-2530.
60. Lacalli, T., *The Middle Cambrian fossil Pikaia and the evolution of chordate swimming.* Evodevo, 2012. **3**(1): p. 12.
61. Gemballa, S. and F. Vogel, *Spatial arrangement of white muscle fibers and myoseptal tendons in fishes.* Comparative Biochemistry and Physiology Part A: Molecular & Integrative Physiology, 2002. **133**(4): p. 1013-1037.
62. Alexander, R.M., *The orientation of muscle fibres in the myomeres of fishes.* Journal of the Marine Biological Association of the United Kingdom, 1969. **49**(2): p. 263-290.
63. Pichitpornchai, C., J.A. Rawson, and S. Rees, *Morphology of parallel fibres in the cerebellar cortex of the rat: an experimental light and electron microscopic study with biocytin.* J Comp Neurol, 1994. **342**(2): p. 206-20.
64. Gundappa-Sulur, G., E. De Schutter, and J.M. Bower, *Ascending granule cell axon: an important component of cerebellar cortical circuitry.* J Comp Neurol, 1999. **408**(4): p. 580-96.
65. Sims, R.E. and N.A. Hartell, *Differences in transmission properties and susceptibility to long-term depression reveal functional specialization of ascending axon and parallel fiber synapses to Purkinje cells.* J Neurosci, 2005. **25**(12): p. 3246-57.
66. Sultan, F. and D. Heck, *Detection of sequences in the cerebellar cortex: numerical estimate of the possible number of tidal-wave inducing sequences represented.* J Physiol Paris, 2003. **97**(4-6): p. 591-600.
67. van Kan, P.L., A.R. Gibson, and J.C. Houk, *Movement-related inputs to intermediate cerebellum of the monkey.* J Neurophysiol, 1993. **69**(1): p. 74-94.

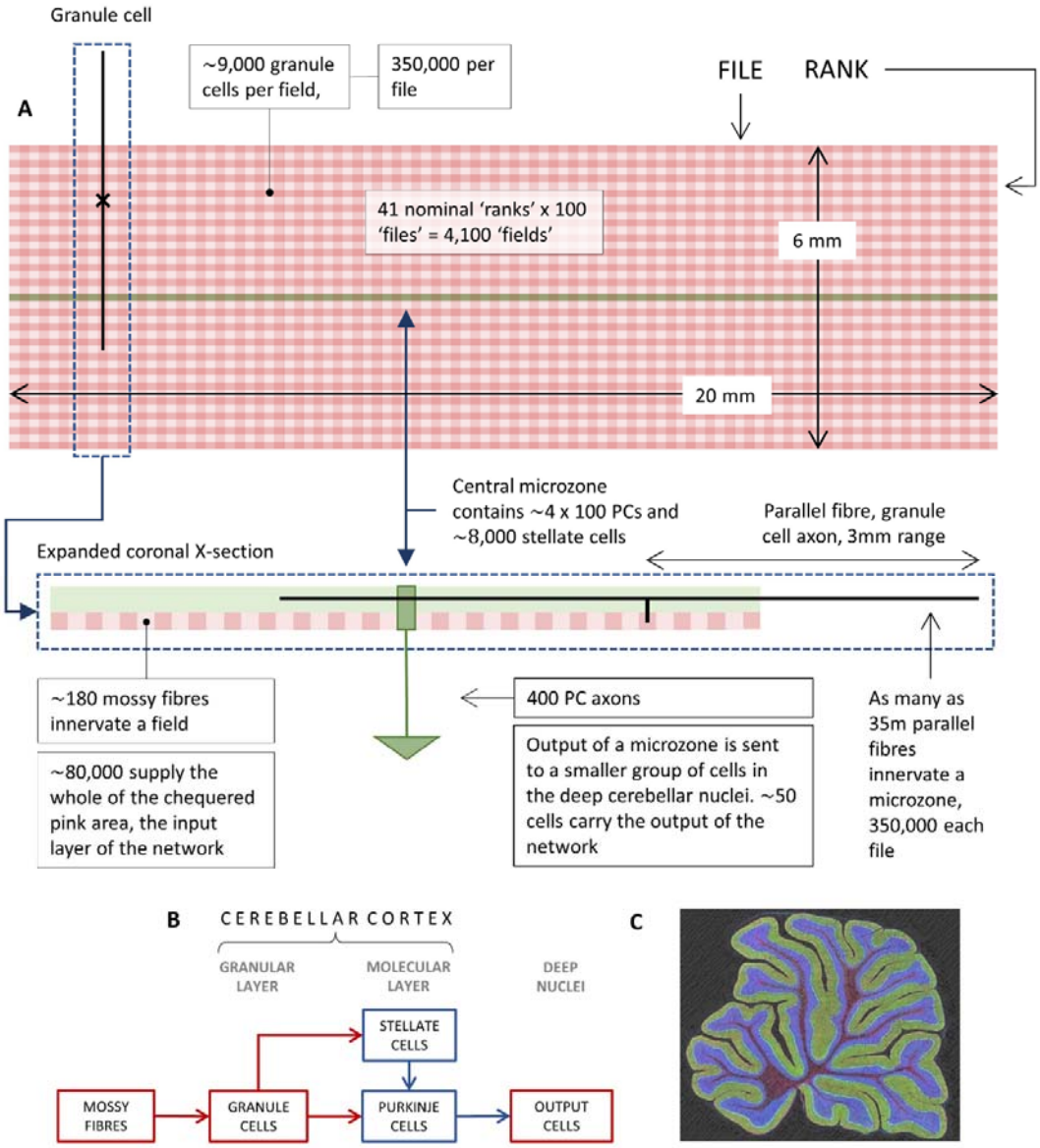


**Fig 1. Graphic of the cerebellar network. A** View of a network from the cerebellar surface, with curvature and folding removed. Relative dimensions are preserved. A microzone (green line, 20 mm x 150 µm, the middle layer of the cerebellar network) equally bisects the region of the granular layer that provides parallel fibre input to it

(chequered area, the input layer), and has output to a discrete cell group in the deep cerebellar nuclei, which includes the output cells of the cerebellum (the output layer). Input to the 'middle microzone' is from 40 'ranks' which lie parallel to it, 20 each side. Ranks are crossed at right angles by 75–100 'files' (100 in this graphic). Each intersection is a 'field'. A field is the average size of a rectangle that encloses a mossy fibre terminal cluster, around 200 x 150 µm [66], sagittal by mediolateral. The granular layer is anatomically seamless; *ranks, files and fields are nominal divisions* which we use to quantify the computational effect of anatomy. They are divisions of the granular layer; microzones are divisions of the molecular layer. Each microzone is the middle layer of its own network. Networks accordingly very substantially overlap anatomically. PCs: Purkinje cells. **Inset** Cross-section: pink: granular layer; pale green: molecular layer; green: middle microzone. **B** Simplified cerebellar circuit wiring, highly preserved across vertebrates. Red: glutamate; blue: GABA. The number of cells of each type in a network (given microzone length of 100 fields) is: 80,000 mossy fibres (not part of the network but supply input) → 35,000,000 granule cells (therefore the number of parallel fibres that innervate the middle microzone) → 8,000 stellate cells → 400 Purkinje cells → 50 output cells. **C** Reproduced with permission of Tom Deerinck. Section of rat cerebellum in the sagittal plane showing cortical layers. Green: molecular layer; blue: granular layer.

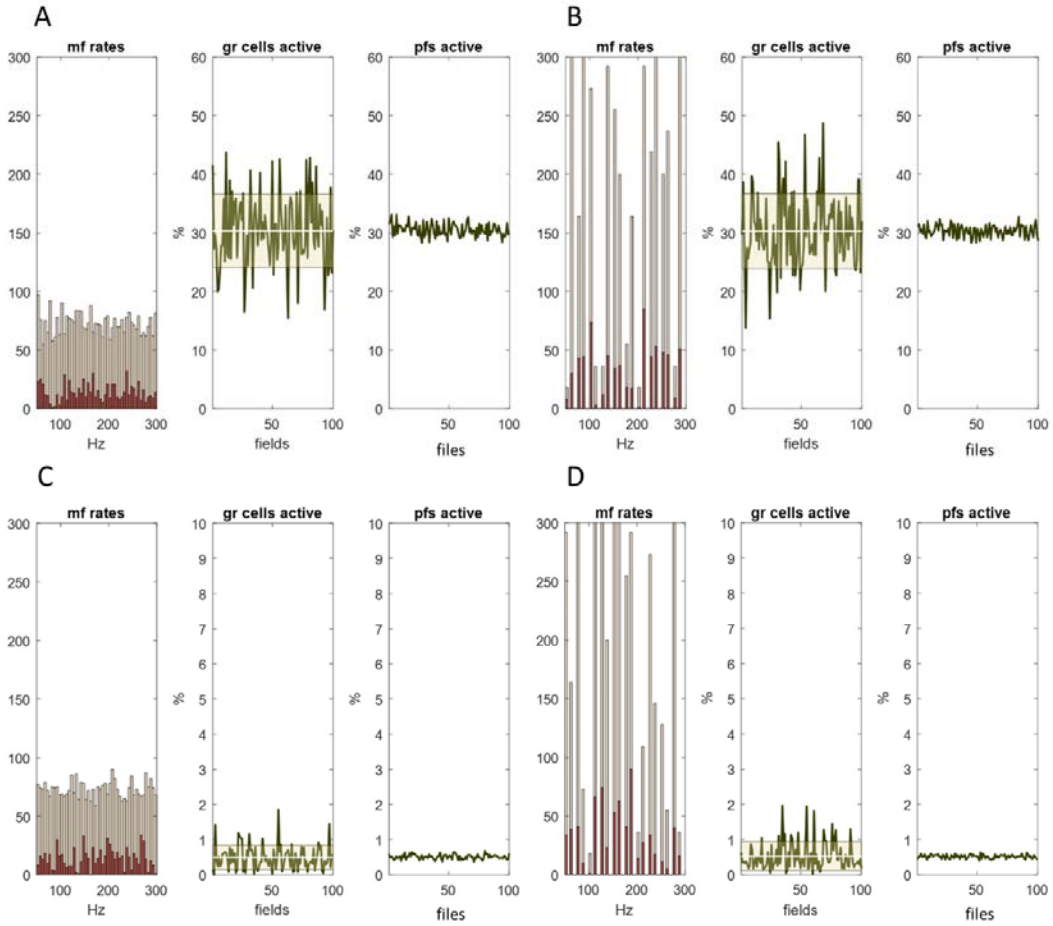


**Fig 2. Recoding in the cerebellar granular layer regulates the fraction of concurrently active parallel fibres.** Recoding in the granular layer regulates the density of active parallel fibres. We ran a simulation of recoding with input to 41 ranks, the input layer of the cerebellar network. The data in the first and fourth columns show, for each simulation, the frequency of mossy fibre input rates to a single rank, selected at random. All ranks in a simulation receive input generated independently and randomly subject to the same constraints on the frequency distribution. The data in the second and fifth columns are the percentage of granule cells that fire in each field of a single rank, again selected at random. The data in the third and sixth columns are the percentage that fire in each file, and therefore the percentage of active parallel fibres

in each file. Regulation is by the pathway mossy fibre → Golgi cell → granule cell, sometimes termed the feed-forward pathway. The simulated mechanism does not include the feedback circuit (mossy fibre → granule cell → Golgi cell → granule cell) traditionally linked to regulation (which provides fine adjustment [40]). The shape of the sampled distribution (columns 1 and 4) does not affect regulation. Top row: ~30% of granule cells are active. Bottom row: Golgi cell inhibition of granule cells is adjusted by a constant so that a lower fraction of granule cells fire, around 0.5%. y axes are scaled to the data so that the contraction of the data range in the bottom row compared to the top is greater than it appears. The range of the percentage of granule cells active in each field (columns 2 and 5) is further narrowed when it is pooled with other fields in a file to give the percentage of active parallel fibres that converge on a microzone (columns 3 and 6).

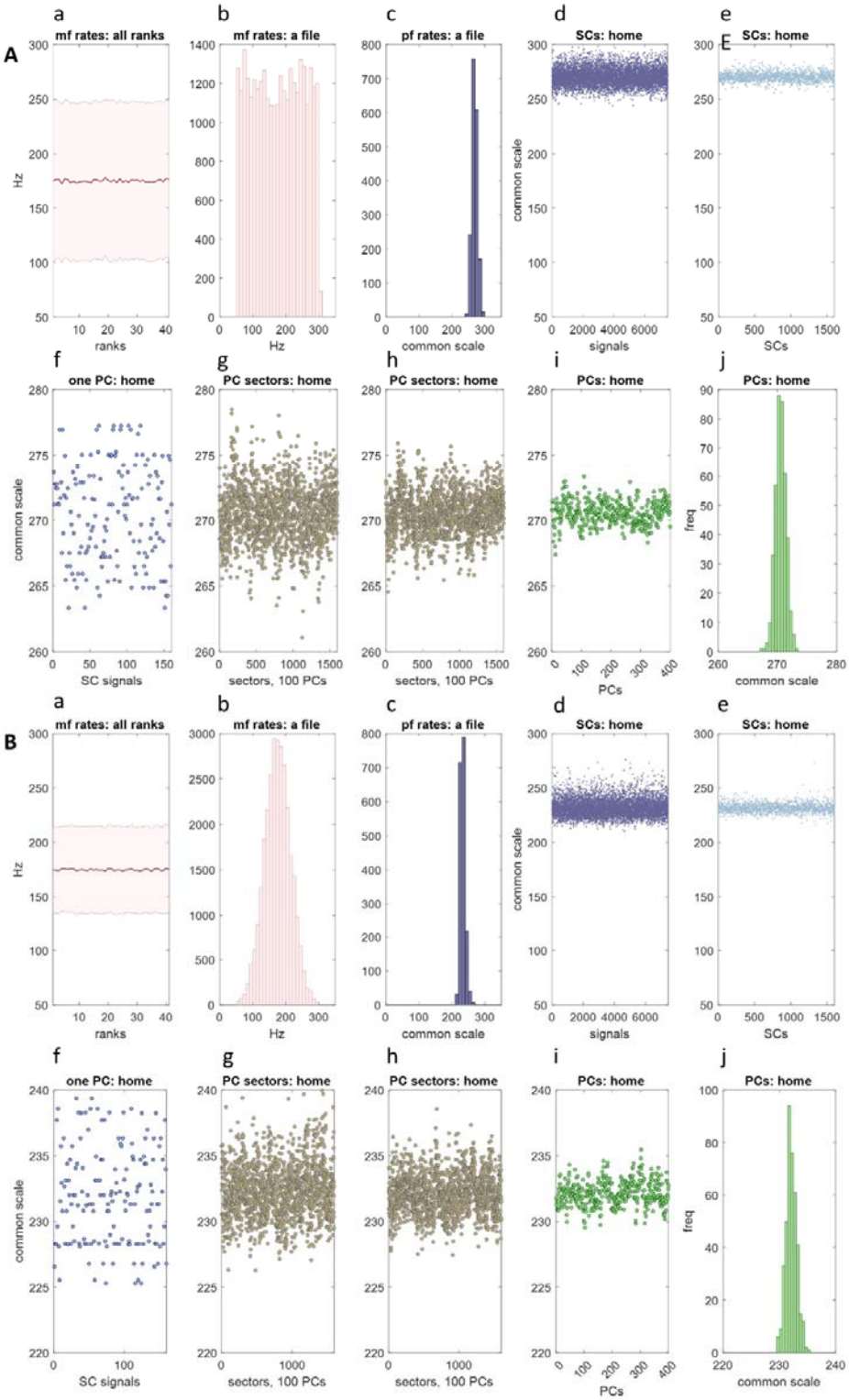
A
a
mf rates: all ranks
Hz
ranks
b
mf rates: a file
Hz
c
pf rates: a file
common scale
d
SCs: home
common scale
signals
e
SCs: home
SCs
f
one PC: home
common scale
SC signals
g
PC sectors: home
sectors, 100 PCs
h
PC sectors: home
sectors, 100 PCs
i
PCs: home
PCs
j
PCs: home
freq
common scale
B
a
mf rates: all ranks
Hz
ranks
b
mf rates: a file
Hz
c
pf rates: a file
common scale
d
SCs: home
common scale
signals
e
SCs: home
SCs
f
one PC: home
common scale
SC signals
g
PC sectors: home
sectors, 100 PCs
h
PC sectors: home
sectors, 100 PCs
i
PCs: home
PCs
j
PCs: home
freq
common scale

**Fig 3. The microzone computation.** Mossy fibre rates are converted into synchronised firing of middle microzone Purkinje cells. mf: mossy fibre; pf: parallel fibre; SC: stellate cell; PC: Purkinje cell. **A. a** We generated a uniform random distribution representing mossy fibre input rates to the entry layer of a cerebellar network using the method described here: [30]. The range, 50–300 Hz, is the typical physiological range for mossy fibres generally [67]. The range received by a network at any given time is probably smaller, and perhaps much smaller, so the range here is chosen to set a hard test for the network computation. Input to each rank was independently and randomly generated within constraints on the frequency distribution. Rate data were then randomly sampled, rank by rank, to derive input rates to each field, and copies added to reflect variable size of mossy fibre terminal clusters, and that most clusters straddle field boundaries, so lie partly inside and partly outside. Red line: mean; pink area: SD. **b** Frequency distribution of mossy fibre rates received by a randomly selected file. As all files cross all ranks, they all receive (to a near approximation) the same frequency distribution of mossy fibre rates. **c** Parallel fibre rates in a randomly selected file. We used the granular layer model [30] to derive the number of granule cells that fire in each field and the rates they each fire at. As all files receive the same frequency distribution of mossy fibre rates, recoding in all files returns the same distribution of granule cell/parallel fibre rates. 0.5% of parallel fibres are active. 'Common scale' means normalised, discussed in the main text. **d** Parallel fibre rates in each file were randomly sampled 80 times, to represent sampling by middle microzone stellate cells. Sample size was a randomly generated (each time a sample was taken) number with Table A probabilities, giving around 7,200 values (16 stellate cells x 100 fields x the weighted mean of distributed probabilities). 'Home' in panel titles refers to the middle microzone. **e** Molecular layer interneurons are reported to reflect 'granule cell input with linear changes in firing rate' [20 p.6]. We took stellate cell firing rates to be the mean of input rates to each cell (hence 1,600 data points). There is a further contraction of the data range. **f** Data represent stellate cell input rates to a single

Purkinje cell. The y-axis range (and in g–i) is shortened (from 250 down to 20). **g** 'Sectors' in the panel title refers to the nominal division of the Purkinje cell dendritic arbour into 16 compartments, each receiving convergent input from a random sample of stellate cells afferent to the cell. Data are the sample means, shown for a single Purkinje cell per field in the middle microzone (so there are 1,600 values, 16 compartments x 1 Purkinje cell x 100 fields). **h** A Purkinje cell receives inhibition from two planar networks of stellate cells, one each side. Step G was repeated, and the data averaged for each compartment. **i** Mean of the compartment means calculated for each Purkinje cell in the middle microzone (so 400 data points, 4 Purkinje cells per field x 100 fields), representing somatic integration of dendritic compartment data. **j** Same data displayed as a histogram (note the x axis range is the same as the y axis in panels f to i, so much shorter than b and c). A uniform distribution of mossy fibre rates with a range of 50–300 Hz in panel a, becomes a very narrow Purkinje cell range, SD < 1 on a normalised scale, with a normal distribution. **B.** We repeated A but with normally distributed mossy fibre rates (SD 40), with the same result. We also obtained the same results (not shown) with a discontinuous mossy fibre distribution (range 50–300 Hz).

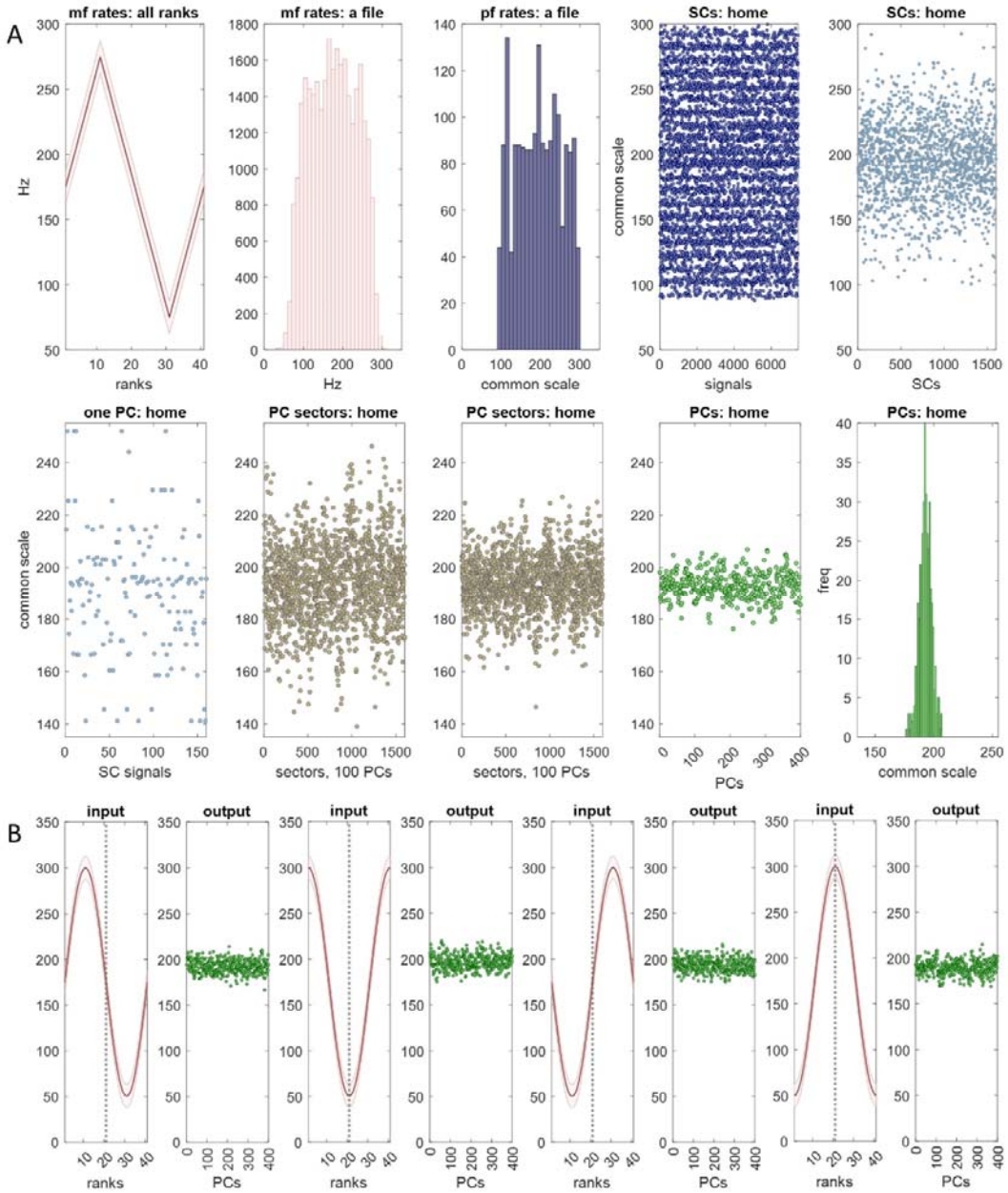


806

807 **Fig 4 Information is coded in the 'shape' of mossy fibre input rates to a network, but**
808 **not in all shapes. A** The same as Fig 3 except that the mean of mossy fibre input rates
809 to each rank changes from rank to rank, so that it has a zig-zag pattern displayed as a

graph. The frequency distribution received by ranks individually is normal and narrow (SD = 12.5 Hz, all ranks). The frequency distribution of mossy fibre rates in a file that crosses at right angles is the same in all files (because they all cross all the same ranks) but not the same as ranks. That impacts on the spread of parallel fibre rates in top row panel 3 and therefore the spread of data in all later panels, so tht Purkinje cell rates (middle row panels 4 and 5) are poorly focussed. The mean of the green data – the output of the microzone computation – still precisely tracks the mean of input rates to the network, as in Fig 3, but, critically, has no relationship with the pattern of input signals frequencies: the zigzag pattern of input frequencies cannot be inferred from green data. The significance is tat the network computation cannot 'decode' the striped pattern of mossy fibre input rates. Note: banding in panel 4 is an artefact of using discrete data sets as input to ranks. Physiological ranks do not have clean boundaries, so the data would merge. **B** We selected the zig-zag pattern as an illustration. However, we moot that the physiological pattern may be sine wave-like, or part of a sine wave, generated by execution of a motor cycle. We test if the computation performs any better if input represents a full cycle. The vertical, dashed line is the position of the middle microzone. Green data are firing rates of Purkinje cells in the middle microzone. Performance does not improve, meaning: Purkinje cell firing rates do not code the striped pattern of mossy fibre firing rates. We advanced the phase of the cycle by 90 degrees each time, but with no effect on Purkinje cell rates.

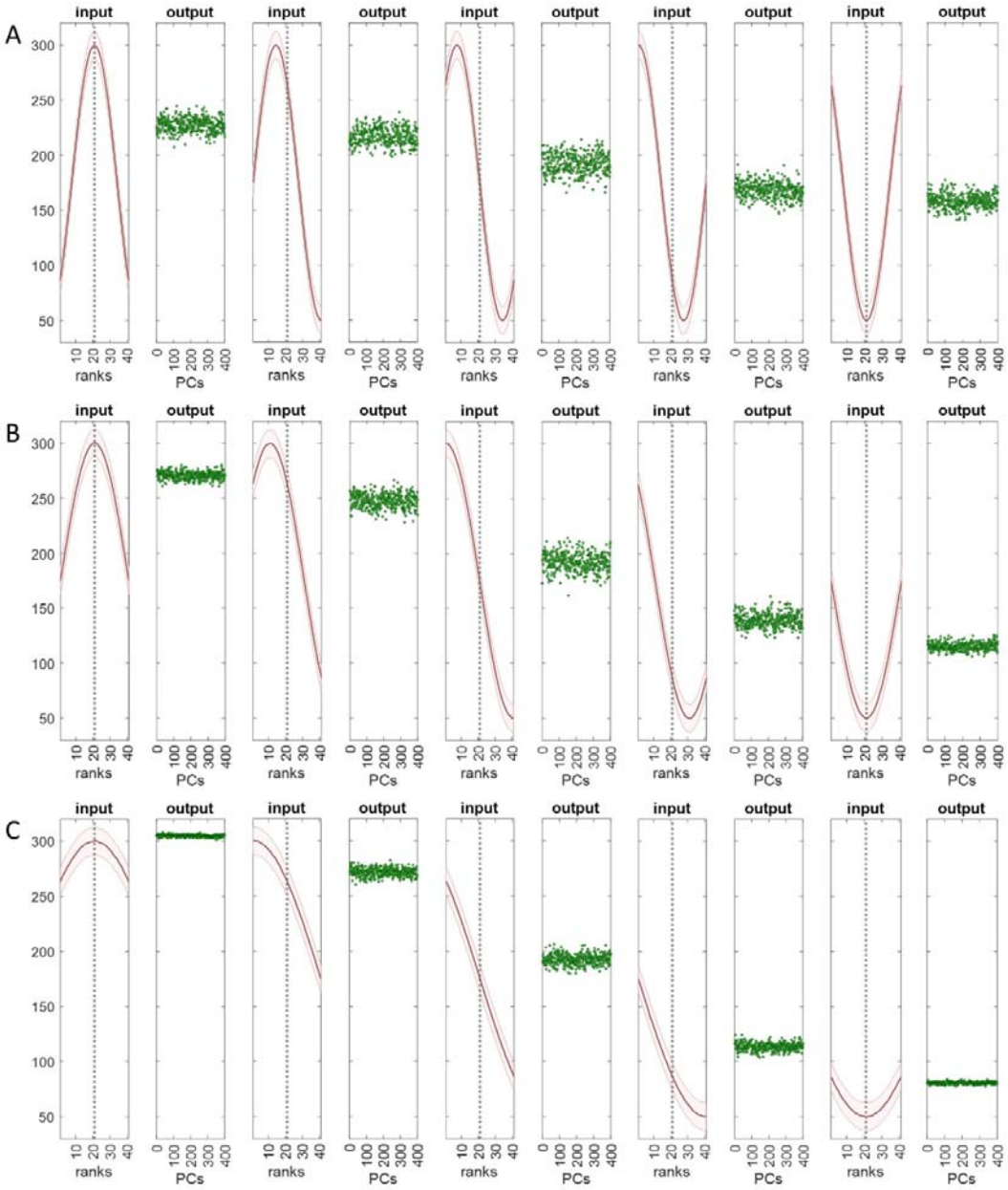


**Fig 5. How does the middle microzone read the striped pattern of mossy fibre input rates to a network?** Phase information becomes readable if input to a network is confined to only part of a cycle. **A** The same as Figure 4B but mossy fibre rates represent 3/4 of a wavelength, phase shifted 45 degrees in each pair of panels. Output

now reflects cycle phase, but the response is insensitive, i.e., output has a modest range compared to the range of mossy fibre rates. Also, Purkinje cell firing is not focussed. **B** The same, but mossy fibre rates represent 1/2 a wavelength. The size of the output range is larger, ~150 normalised 'Hz', twice the range in A. Purkinje cell data are more focussed. **C** Mossy fibre rates represent 1/4 of a wavelength. The bandwidth of the output range increases again, to almost the mossy fibre range. That is, output reliably and precisely codes phase information. Purkinje cell firing rates are most focussed. The smaller the fraction of a wavelength that mossy fibre signals code, the more sensitive and precise the information coded collectively by Purkinje cells.